

Unsupervised Person Re-identification via Simultaneous Clustering and Consistency Learning

Junhui Yin, Jiayan Qiu, Siqing Zhang, Jiyang Xie, Zhanyu Ma*, and Jun Guo

Abstract

Unsupervised person re-identification (re-ID) has become an important topic due to its potential to resolve the scalability problem of supervised re-ID models. However, existing methods simply utilize pseudo labels from clustering for supervision and thus have not yet fully explored the semantic information in data itself, which limits representation capabilities of learned models. To address this problem, we design a pretext task for unsupervised re-ID by learning visual consistency from still images and temporal consistency during training process, such that the clustering network can separate the images into semantic clusters automatically. Specifically, the pretext task learns semantically meaningful representations by maximizing the agreement between two encoded views of the same image via a consistency loss in latent space. Meanwhile, we optimize the model by grouping the two encoded views into same cluster, thus enhancing the visual consistency between views. Experiments on Market-1501, DukeMTMC-reID and MSMT17 datasets demonstrate that our proposed approach outperforms the state-of-the-art methods by large margins.

1. Introduction

Convolutional Neural Networks (CNNs) have undergone unprecedented success in visual representation learning recently. To realize rich representation, CNNs are typically trained using large-scale datasets (e.g., ImageNet [8]) with extensive human annotations. Despite their success, the large-scale data annotation is costly and laborious, especially for complex data (e.g., videos) and concepts (e.g., image retrieval [7, 25, 45]). In contrast to the methods [23, 19] that rely on heavy supervision, self-supervised learning is another kind of technique, which can easily obtain the supervision signal from the data itself and employ it to facilitate representation learning without requiring extensive human annotation supervision.

A fertile source of annotation-free supervision is video since the visual world is continuous and does not change abruptly. Based on this, [37] uses inherent consistency be-

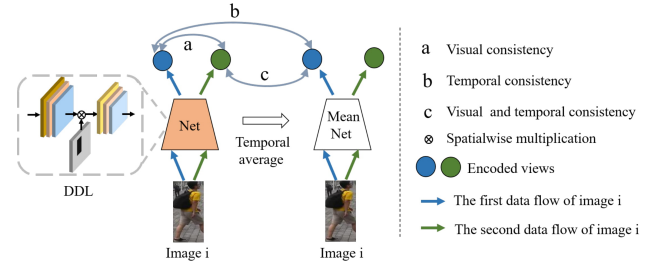


Figure 1: a: Visual consistency from two different encoded views of the same image based on network with Dynamic dropblock layer (DDL). b: Temporal consistency from the same encoded view at different stages (i.e., iterations). c: Visual and temporal consistency from different views at different stages.

tween observations adjacent in time as free supervisory information for training model. Learning consistency meets the development of the human visual system as infants can track and follow slow-moving objects before mapping objects to semantic meanings. In this work, we focus on constructing consistency in still person images for unsupervised representation learning under the framework of person re-identification (re-ID).

The requirement of re-ID is to match a person of interest with other images of this person from non-overlapping cameras. Existing unsupervised re-ID approaches [12, 27] first extract embedding features of unlabeled dataset from network model and then apply unsupervised clustering to divide images into different clusters for training model. These methods generate pseudo labels as ground-truth labels by simply using clustering algorithm and thus have not yet fully explored the semantic information existing in data itself, which limits representation capabilities of learned models. In addition, the current clustering-based methods only focus on target task of re-ID and easily latch onto local information and low-level features (e.g., color, contrast, texture, etc.), which is unwanted for the objective of semantic clustering [35].

To address the above problems, we design a pretext task for unsupervised re-ID by learning consistency from still

images, such that the clustering network can separate the images into semantic clusters rather than focusing on low-level features. Similar to previous unsupervised representation learning [37, 38], the aim of **Consistency Learning** (ConsLearn) is to learn feature representations that support reasoning at visual and temporal consistency. To construct the consistent information from single image and turn them into a learning signal for optimizing network, we first propose Dynamic Dropblock Layer (DDL), which randomly drops the region of input maps, namely the semantic body parts, to obtain differently semantical representations based on the attentive feature learning of remaining regions. Then, we feed the same person image into the model twice and apply DDL to convolutional feature maps of the model to produce two encoded views (*i.e.*, feature representations) of the image. Finally, the consistency across views is ensured by maximizing agreement between two encoded features via a consistency loss in latent space. The motivation behind ConsLearn lies in that there is inherent visual consistency between the different views of the same images in space and the predicted target region of training image can still backtrace to the initial information by using the information of the other view regardless of losing the target on a view.

The above pretext task integrates disparate visual percepts into persistent entities and enhances visual consistency in feature space. To further enhance the temporal consistency across different training stages (*i.e.*, iterations), we improve on existing methods by adopting the temporal average model of network from the previous iterations to generate the invariance feature for a view of image, which enables the consistency with the other view obtained by the current encoder model, as shown in Figure 1.

Simultaneous clustering and consistency learning is one of the most promising approaches for unsupervised learning of deep neural networks. As a pretext task, ConsLearn can obtain the free supervision for consistency from the unlabeled data and learn feature representations that supports identifying consistency across views. As these features improve, the ability to predict the missing patch of feature maps are enhanced, inching the model toward consistency. As a target task, clustering process trains a deep neural network using pseudo-labels and encourages network model to focus on the current task of re-ID. The self-supervised task from representation learning requires semantic understanding and thus induces clustering to obtain semantically meaningful features rather than depending on low-level features, which is present in existing clustering-based approaches [12, 27, 13].

The main contributions of this work can be summarized as follows:

- A novel **Consistency Learning** (ConsLearn) approach is proposed to construct data association across encoded views from unlabeled pedestrian images and learn represen-

tations for visual reasoning in a self-supervised manner.

- ConsLearn is implemented with clustering, which not only perceives the current pretext task, but also learns the feature information related to the target task. In this way, our method can automatically separate images into semantically meaningful clusters.

- The proposed method is applied on unsupervised person re-ID and further extended to unsupervised domain adaptation (UDA) re-ID, and improves the state-of-the-arts with significant margins.

2. Related Work

Unsupervised person re-identification. Unsupervised person re-identification (re-ID) is very challenging to learn discriminative representation due to the absence of target labels as learning guidance. Several methods [12, 27, 46] resort to separate unlabeled data into different clusters by clustering algorithms (*e.g.*, DBSCAN [11]) and iteratively trains network models based on the generated pseudo labels. However, these methods highly rely on pseudo labels and may be affected due to the hard quantization error caused by the clustering error. To address this issue, some existing methods use some weak supervised signal for training re-ID model. For instance, the tracklet-based method [24] uses person tracklet as supervised information to jointly learning within-camera tracklet correlation and cross-camera tracklet association, without any additional annotations. Despite their success, these methods are not truly unsupervised learning in essence and work hard when there are not labeled data and weak supervised information (*e.g.*, tracklet). Another line of this work is to employ deep re-ID model learned from labeled source data as an initialized feature extractor and adapt the model with both source domain and target domain to reduce the domain discrepancy between different datasets on image-level [9, 39, 2] and attribute feature-level [29, 6]. [14] and [48] use multiple network models and their corresponding mean nets to generate soft pseudo labels for supervising other models. The main difference from them is that we construct temporal consistency during training process by only using one current network and its past (mean) network with DDL. In addition, many other contrastive learning methods [18, 15] also using the momentum-based averaging model.

Self-supervised representation learning. As a form of unsupervised learning, self-supervised representation learning is a kind of techniques that learn representations by solving a pretext task, where the supervision signal can be obtained freely from the large amount of unlabeled data available online. Contrastive learning [16] is the core idea in this line of investigation. It has recently shown great progress [40, 33, 20, 1, 43]. As a milestone, MoCo [18] maintains a queue of negative samples and train the model with a memory bank to improve consistency of the queue.

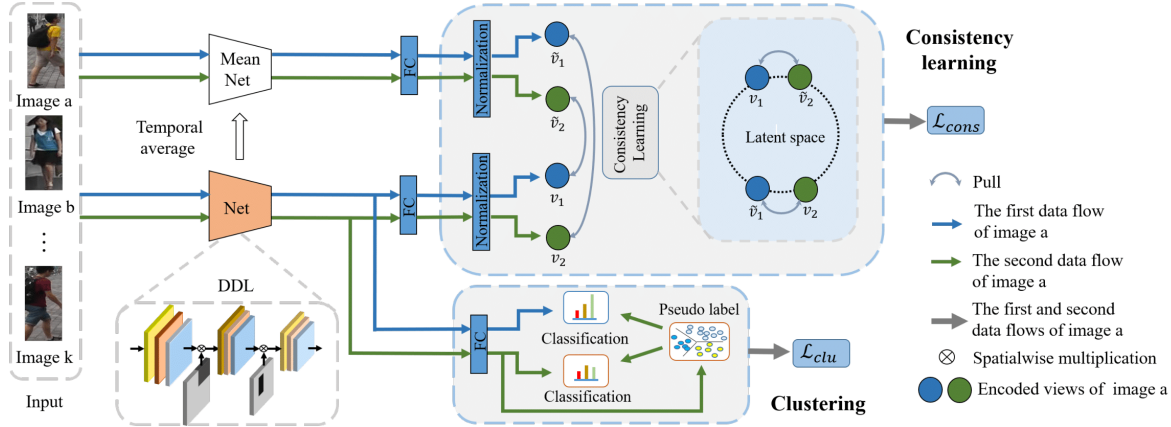


Figure 2: Illustration of our proposed framework. During training, unlabeled data are fed-forward into the deep re-ID network with DDL and its temporally averaging model to obtain differently encoded views (*i.e.*, feature representations). Subsequently, two components are designed to optimize the network with unlabeled data, respectively. The first component is a clustering module that provides the same cluster assignments for two encoded features to calculate the cross-entropy loss. The second component is ConsLearn module that learns vision and temporal consistency from still images via a consistency loss.

After that, considerable attention has been focused in this direction [5, 34, 3, 15, 4] and spread over many other tasks [42, 17]. Inspired by MoCo series [18, 5], we use the mean net to construct temporal consistency during training process. Different from these works, our method is The main difference from MoCo series [18, 5] is our method can be thought of as MoCo without negatives and rarely depend on large batch, while MoCo highly relies on them.

Compared to still images, videos should be a fertile source for self-supervised learning as they naturally possess the temporal resolution and dynamics. A suitable supervision for free is inherent visual correspondence between adjacent frames in video. [37] utilizes cycle consistency as free supervision to learn fine-grained correspondences between pixels. [38] propose a data association method, which concentrates more on learning high-level semantic correspondences and is adaptive to the re-ID problem. However, this technique is required to the prior knowledge of camera view labels, which sometimes are unavailable. The above methods usually focus on learning consistency between adjacent frames of video, while ours concentrate more on how to find the consistency in still person images and utilize it to provide a self-supervised solution for person re-ID task, without any additional information (*e.g.*, camera view labels).

3. Approach

In this section, we first propose the consistency learning (ConsLearn) as a pretext task for unsupervised person re-ID. We then introduce the discriminative clustering method and incorporate it with ConsLearn in a joint optimization

framework. The overview of the training procedure is illustrated in Figure 2.

3.1. Consistency Learning

Clustering tends to focus on low-level features, like color, which is unessential for the objective of semantic clustering. To explore richer visual patterns and obtain semantically meaningful features, we propose ConsLearn and integrate it with the clustering network. The following sections present the cornerstones of our approach, which can encourage clustering network to separate images into semantically meaningful clusters without human annotations.

Dynamic dropblock layer. In this subsection, we present the details of dynamic dropblock layer (DDL). DDL can be applied on any feature layer of network model, and induce model to capture the different semantic information of the object during training. It is worth noting that DDL is deactivated during the testing phase.

The input of DDL is a convolutional feature map $F \in \mathbb{R}^{H \times W \times C}$ where C represents the number of channels, H and W are height and width of feature map, respectively. We first set two main hyperparameters α and β . They control the height and width ratio of the erased region on map F , respectively. The size of region to be dropped increases as α and β increases and is adaptive to the size of feature map when the hyperparameters are fixed. Therefore, the dropblock layer is dynamic. The height and width of the erased region vary from task to task. But in our work, the removed region should contain a semantic part of feature map. Specifically, the drop mask $M_{drop} \in \mathbb{R}^{H \times W}$ is generated by setting the pixel to 0 if it is inside the generated erased region, and 1 otherwise. The DDL randomly remove the part

of feature map F by multiplying it to the drop mask. In this way, we can produce different views for input feature map, namely different semantic body parts. We visualize the example of each component in the following experiment. The regularization technique of Cutout [10] also studies the application of random erasing. A difference from Cutout is the erased region size of our DDL changes dynamically with the size of feature map, while the removed region size of Cutout is fixed and squared. The other difference is that our DDL can be applied on any feature layer of network instead of only input image as in Cutout. In fact, our DDL can be considered as an extension of random erasing for feature maps and also an extension of Cutout [10] or Dropout [32].

Learning consistency. Consider as input a person images x , the pixel input is mapped to a feature space twice by an encoder with DDL, such that $h_k = \Phi_k(x|\theta)$, $k = 1, 2$. Here, $k = 1, 2$ mean the two data flows of the same image, which are fed into network in order. Since the erased area of DDL is given randomly at each layer, the firstly entered network $\Phi_1(\cdot|\theta)$ is different from the second network $\Phi_2(\cdot|\theta)$. Thus, k is also used to distinguish them. This is also why we use two data flows for the same image. In this way, the network models $\Phi_k(\cdot|\theta)$ output two different encoded views h_k , $k = 1, 2$, leading to two differently semantic features from the same image. Our aim is to reduce the ability for clustering depending on low-level features and induce the model to learn the inherent visual consistency across different views. Therefore, we want to maximize the agreement between h_1 and h_2 . A linear layer $g: \mathbb{R}^D \rightarrow \mathbb{R}^\Omega$ follows the feature representations to map them to a latent space, which is defined as

$$u_k = g(h_k), k = 1, 2. \quad (1)$$

In this space, our model can better learn a semantically meaningful representation that describes what is in common between u_1 and u_2 while discarding instance-specific details.

The encoder model at current iteration can output the encoded views for all the person images, but this rapidly changing encoder also reduces the feature representations' consistency across different training stages and eventually results in training error amplification. To resolve this issue, we present the momentum-based moving average model as a way of preserving more original knowledge for unsupervised learning with a consistency loss. Formally, let the temporal average model be $\Phi_k^*(\cdot|\theta^*)$. Then, its model parameter $\theta^{*(t)}$ at current iteration t can be updated by

$$\theta^{*(t)} = \zeta\theta^{*(t-1)} + (1 - \zeta)\theta^{(t)}, \quad (2)$$

where $\zeta \in [0, 1)$ is a momentum coefficient and the initial temporal average parameters $\theta^{*(0)}$ is θ .

Two momentum-based encoded views of the same images are generated by the temporal average model ϕ and the

linear layer g^* . That is, $\tilde{u}_k = g_k(\Phi_k^*(x_k))$, $k = 1, 2$. Considering the errors caused by self-variation and large differences in values, the feature distributions u_k and \tilde{u}_k are scaled up by a softmax operation,

$$v_{kl} = \delta(u_k) = \frac{e^{u_{kl}}}{\sum_{j=1}^{\Omega} e^{u_{kj}}}, k = 1, 2, \quad (3)$$

$$\tilde{v}_{kl} = \delta(\tilde{u}_k) = \frac{e^{\tilde{u}_{kl}}}{\sum_{j=1}^{\Omega} e^{\tilde{u}_{kj}}}, k = 1, 2, \quad (4)$$

where $v_{kl}(\tilde{v}_{kl})$ is the l -th element of $v_k(\tilde{v}_k)$. Now, the problem is how to turn the consistency information into a learning signal for optimizing network models.

It is well known that the Kullback-Leibler (KL) divergence $KL(\cdot)$ can be thought of as a measurement of how far the distribution Q is from the distribution P . For discrete probability distributions P and Q defined on the same probability space \mathcal{X} , P typically represents the "true" distribution of data, while Q typically represents an approximation of P . In order to find a distribution Q that is closest to P , we can minimize KL divergence, which can be rewritten by

$$\begin{aligned} KL(P||Q) &= - \sum_{x \in \mathcal{X}} P(x) \log(Q(x)) + \sum_{x \in \mathcal{X}} P(x) \log(P(x)) \\ &= H(P, Q) - H(P), \end{aligned} \quad (5)$$

where $H(P, Q)$ is the cross entropy of P and Q , and $H(P)$ is the entropy of P . Here, $KL(P||Q)$ is proportional to $H(P, Q)$ if $H(P)$ is a constant.

The embedding features v_k and \tilde{v}_k , $k = 1, 2$, can be interpreted as the distribution of a discrete random variable over training samples x . Furthermore, \tilde{v}_i can be viewed as a constant or "true" distribution since it represents invariant feature distribution obtained by the temporally moving average model. Our aim is that v_1 should be close to \tilde{v}_2 and v_2 should be close to \tilde{v}_1 as much as possible, which supports visual reasoning between different semantic features. Therefore, $H(P, Q)$ is adopted to turn the consistency information into a learning signal for optimizing our models. The consistency of different encoded views is measured using the following loss, as

$$\begin{aligned} \mathcal{L}_{co} &= H(\tilde{v}_1, v_2) + H(\tilde{v}_2, v_1) \\ &= - \sum \tilde{v}_1 \log(v_2) - \sum \tilde{v}_2 \log(v_1). \end{aligned} \quad (6)$$

3.2. Unsupervised Person Re-identification by Clustering

Unlike pervious clustering techniques [12, 27, 13], our clustering method first generates pseudo labels according to features from a view of the same images and utilizes the same labels for all the encoded views since they share large visual similarity. Its aim is to further enhance the visual consistency between different views based on unsupervised

clustering. Specifically, given encoded features $\{h_1^i\}_{i=1}^N$ of images $\{x^i\}_{i=1}^N$ from a view, clustering algorithm (*i.e.*, DBSCAN [11]) divides these learned features into different clusters as pseudo label $\{\hat{y}_i\}_{i=1}^N$, which represents the image’s membership to one of M possible predefined categories. Meanwhile, the representations are also fed into a linear classification layer, converting the feature vector h_1^i into a vector of class scores z_1^i . Finally, the softmax operator is performed to map the class scores to class probabilities $p(\hat{y}_i|x_i)$, which is the predicted probability of image x_i belonging to the identity \hat{y}_i . As in [52], the clustering procedure for two encoded views is achieved by minimizing the cross entropy loss,

$$\mathcal{L}_{ce} = -\frac{1}{N} \sum_{i=1}^N \log p(\hat{y}_i|h_1^i) - \frac{1}{N} \sum_{i=1}^N \log p(\hat{y}_i|h_2^i). \quad (7)$$

Furthermore, we introduce a softmax-triplet loss to enforce a positive pair to be closer and a negative pair apart from each other in the representation space. As in [21], let $h_1^{(in)}$ and $h_1^{(ip)}$ denote the similarity of the hardest negative pair $\{h_1^i, h_1^n\}$ and the hardest positive pair $\{h_1^i, h_1^p\}$ for encoded views $\{h_1^i\}_{i=1}^N$, with an anchor h_1^i . The similarity can be computed as $h_1^{(in)} = -\|h_1^i - h_1^n\|$ and $h_1^{(ip)} = -\|h_1^i - h_1^p\|$, where $\|\cdot\|$ represents Euclidean distance. In this sense, minimizing the similarity of the hardest negative pair means maximizing the distance between $h_1^{(i)}$ and $h_1^{(n)}$ and vice versa. Similarly, encoded views $\{h_2^i\}_{i=1}^N$ have similar results. Thus, the softmax-triplet loss for two encoded views can be performed by

$$\begin{aligned} \mathcal{L}_{st} = & -\frac{1}{N} \sum_{i=1}^N \log \frac{\exp(h_1^{(in)})}{\exp(h_1^{(in)}) + \exp(h_1^{(ip)})} \\ & -\frac{1}{N} \sum_{i=1}^N \log \frac{\exp(h_2^{(in)})}{\exp(h_2^{(in)}) + \exp(h_2^{(ip)})}. \end{aligned} \quad (8)$$

Overall, unsupervised deep clustering alternates between clustering features as pseudo label to update the parameters of the model using Eq. (7) and learning features by collecting and distinguishing informative pairs accurately using Eq. (8). The proposed procedure can be achieved by

$$\mathcal{L}_{clu} = \lambda \mathcal{L}_{ce} + \xi \mathcal{L}_{st} \quad (9)$$

The overall loss for network. ConsLearn is implemented with clustering, which not only perceives the current pretext task, but also learns the feature information related to the target task. By adding the clustering loss (Eq. (9)) into the consistency loss (Eq. (6)), the overall loss \mathcal{L} of our final proposed method can be expressed as

$$\mathcal{L} = \lambda \mathcal{L}_{ce} + \xi \mathcal{L}_{st} + \eta \mathcal{L}_{co}, \quad (10)$$

where λ , ξ and η are weighting parameters.

| Methods | Market | | Duke | | MSMT17 | |
|------------|-------------|-------------|-------------|-------------|-------------|-------------|
| | mAP | top-1 | mAP | top-1 | mAP | top-1 |
| OIM [41] | 14.0 | 38.0 | 11.3 | 24.5 | - | - |
| BUC [27] | 38.3 | 66.2 | 27.5 | 47.4 | - | - |
| SSL [28] | 37.8 | 71.7 | 28.6 | 52.5 | - | - |
| MAR [44] | 40.0 | 67.7 | 48.0 | 67.1 | - | - |
| TAUDL [12] | 43.5 | 61.7 | 41.2 | 63.7 | 12.5 | 28.4 |
| MMCL [36] | 45.5 | 80.3 | 40.2 | 65.2 | 11.2 | 35.4 |
| HCT [46] | 56.4 | 75.2 | 45.1 | 63.2 | - | - |
| CycAs [38] | 64.8 | 84.8 | 60.1 | 77.9 | - | - |
| MMT* [14] | 74.7 | 88.4 | 60.8 | 75.0 | 25.8 | 57.2 |
| Ours | 77.7 | 90.4 | 64.5 | 78.1 | 27.7 | 55.5 |

Table 1: Comparisons with state-of-the-art methods on three benchmarks for unsupervised person re-ID task. “*” means the results are reproduced by implementing the authors’ code. Bold text refers the best performance.

4. Experiments and Discussions

4.1. Experimental Settings

Datasets and evaluation protocol. Our proposed model is evaluated on three public person re-identification (re-ID) benchmarks: Market-1501 [50], DukeMTMC-reID [31], and MSMT17 [39]. To evaluate the performance of our method, two evaluation metrics are chosen as the mean Average Precision (mAP) and the cumulative matching characteristic (CMC) top-1, top-5, top-10 accuracies [50].

Implementation details. All person images are resized to 256×128 before fed into the networks. Then, we adopt random cropping and flipping as the data augmentation. After that, we feed these images into ResNet-50 [19] with the last classification layer removed, initialized by the ImageNet [8]. We use a mini-batch size of 256 in 4 GPUs. The network models are trained for 50 epochs, using ADAM optimizer with learning rate of 0.00035, weight decay of 0.0005. DBSCAN [11] is used for clustering in each epoch. For the momentum coefficient, we set ζ as 0.999. We empirically set the hyperparameters λ , ξ and η for loss balance as 0.2, 0.35 and 0.1 for unsupervised re-ID on benchmarks including Market-1501 and DukeMTMC-reID. For other datasets, these parameters may be slightly different.

4.2. Comparisons with State-of-the-arts

Unsupervised person re-identification. To verify effectiveness of the proposed method, we compare our method with the state-of-the-art methods by training the re-ID model without any labeled data. Table 1 shows the experimental results on three benchmarks, including Market-1501 (Market), DukeMTMC-reID (Duke), and MSMT17. On Market-1501, under the same setting, our method achieves the best performance among the compared methods with $mAP=77.7\%$ and $top-1=90.4\%$, which exceeds

| Methods | Duke → Market | | | Market → Duke | | |
|-----------------|---------------|-------------|-------------|---------------|-------------|-------------|
| | mAP | top-1 | top-5 | mAP | top-1 | top-5 |
| PUL [12] | 20.5 | 45.5 | 60.7 | 16.4 | 30.0 | 43.4 |
| SPGAN [9] | 22.8 | 51.5 | 70.1 | 22.3 | 41.1 | 56.6 |
| HHL [51] | 31.4 | 62.2 | 78.8 | 27.2 | 46.9 | 61.0 |
| UCDA [30] | 30.9 | 60.4 | - | 31.0 | 47.7 | - |
| PDA-Net [26] | 47.6 | 75.2 | 86.3 | 45.1 | 63.2 | 77.0 |
| CR-GAN [6] | 54.0 | 77.7 | 89.7 | 48.6 | 68.9 | 80.2 |
| PCB [49] | 54.6 | 78.4 | - | 54.3 | 72.4 | - |
| SSG [13] | 58.3 | 80.0 | 90.0 | 53.4 | 73.0 | 80.6 |
| ECN++ [53] | 63.8 | 84.1 | 92.8 | 54.4 | 74.0 | 83.7 |
| MMCL [36] | 60.4 | 84.4 | 92.8 | 51.4 | 72.4 | 82.9 |
| SNR [22] | 61.7 | 82.8 | - | 58.1 | 76.3 | - |
| AD-Cluster [47] | 68.3 | 86.7 | 94.4 | 54.1 | 72.6 | 82.5 |
| MMT [14] | 71.2 | 87.7 | 94.9 | 65.1 | 78.0 | 88.8 |
| DG-Net++ [54] | 61.7 | 82.1 | 90.2 | 63.8 | 78.9 | 87.8 |
| MEB-Net [48] | 76.0 | 89.9 | 96.0 | 66.1 | 79.6 | 88.3 |
| Ours | 82.2 | 92.7 | 96.9 | 68.3 | 80.9 | 90.2 |

Table 2: Comparisons with state-of-the-art methods on Dukemtmc-reID (Duke) and Market-1501 (Market) for domain adaptive tasks.

the state-of-the-art method (MMT [14]) by large margins (3.0% for mAP and 2.0% for top-1). On DukeMTMC-reID, we also achieve evident 3.7% mAP improvement over the current best approach. For a larger and more challenging dataset (MSMT17), the proposed method has also achieved comparable performance in terms of mAP and CMC. With the obtained results, we validate that our method is able to learn richer representations of person images compared with previous methods.

Unsupervised domain adaptation person re-identification. To further demonstrate its effectiveness, our method is tested on several domain adaptation tasks, which are the representative target tasks to validate the effectiveness of unsupervised representation. These tasks contains Duke-to-Market and Market-to-Duke. We initialize the backbone with the model pre-trained on labeled source domain, and fine-tune on unlabeled target domain.

Table 2 summarizes the experimental results on two adaptation tasks. On Market-to-Duke, compared to the state-of-the-art method, our method obtains 6.2% and 2.8% improvements on mAP and Top-1 accuracy, respectively. Similar results can be observed in Market-to-Duke. The above impressive performances demonstrate the necessity and effectiveness of our proposed method for unsupervised domain adaptation re-ID. More importantly, current advanced techniques (MMT [14] and MEB-Net [48]) train multiple networks to enhance the discrimination capability of re-ID model, while our method only use a network and thus is not required for the additional learning parameters in training stage compared to MMT and MEB-Net.

| Applied stage | mAP | top-1 | top-5 | top-10 |
|-----------------------------|-------------|-------------|-------------|-------------|
| $stage_{\{0\}}$ | 63.0 | 77.7 | 87.3 | 90.6 |
| $stage_{\{1, 3\}}$ | 63.3 | 77.8 | 87.5 | 90.7 |
| $stage_{\{0, 1, 2\}}$ | 64.5 | 78.1 | 87.8 | 90.9 |
| $stage_{\{0, 1, 2, 3, 4\}}$ | 61.8 | 75.9 | 85.8 | 89.8 |
| $stage_{\{2, 3, 4\}}$ | 59.3 | 75.3 | 84.9 | 88.3 |
| $stage_{\{2, 4\}}$ | 58.4 | 74.7 | 84.7 | 87.7 |
| $stage_{\{3, 4\}}$ | 57.7 | 74.3 | 84.2 | 87.2 |
| N/A | 54.2 | 72.0 | 81.3 | 85.1 |

Table 3: Effects in performance upon the choice of the feature maps to employ DDL. $stage_{\{0, 1, 2\}}$ refers that DDL is plugged into network before the intermediate stages: $stage_0$, $stage_1$, and $stage_2$, and others are similar. N/A indicates that DDL outputs the raw input feature map instead of applying DDL.

| Applied stage | (α, β) | mAP | top-1 | top-5 |
|-----------------------|-------------------|-------------|-------------|-------------|
| $stage_{\{0, 1, 2\}}$ | (0.2,0.1) | 56.0 | 73.0 | 82.9 |
| | (0.3,0.2) | 60.6 | 75.9 | 86.0 |
| | (0.4,0.3) | 64.5 | 78.1 | 87.8 |
| | (0.5,0.4) | 56.4 | 71.2 | 83.1 |
| $stage_{\{3, 4\}}$ | (0.2,0.1) | 55.4 | 72.4 | 82.4 |
| | (0.3,0.2) | 56.8 | 73.9 | 84.0 |
| | (0.4,0.3) | 57.7 | 74.3 | 84.2 |
| | (0.5,0.4) | 55.8 | 73.0 | 83.3 |

Table 4: Accuracies according to the size (α, β) of the erased region. Upper: Accuracies with DDL deactivated. Middle: Accuracies when DDL applied for lower-level layers. lower: Accuracies when DDL applied for higher-level layers.

4.3. Ablation Studies

In this section, we conduct extensive experiments on DukeMTMC-reID to analyze the effect of our method under different setting.

Dynamic dropout layer. First, we explore the influence of DDL at different stages by integrating DDL into ResNet-50. During the training phase, we plug DDL into network before the intermediate stages: stage 0, stage 1, stage 2, stage 3, and stage 4. For instance, stage 0 means that DDL is plugged into network before input map is fed into network. Table 3 reports the experimental results. From these results, it can be observed that the best accuracy can be achieved when the DDL is plugged in lower-level layers. However, the performance of DDL becomes worse under higher-level layers. The reason behind is that first-layer features are typically more general (e.g., unrelated to a particular task) while last-layer features exhibit greater levels of specificity (e.g., semantic and appearance diversity). This indicates that DDL tends to work if the features are general, meaning suitable to both pretext task and

| Method | \mathcal{L}_{ce} | \mathcal{L}_{st} | DDL | \mathcal{L}_{co} | mAP | top-1 |
|----------------------|--------------------|--------------------|-----|--------------------|-------------|-------------|
| Baseline | ✓ | | | | 53.0 | 71.6 |
| | ✓ | ✓ | | | 55.7 | 73.6 |
| Clustering | ✓ | | | | 50.3 | 69.3 |
| | ✓ | ✓ | | | 54.0 | 73.4 |
| Baseline+ConsLearn | ✓ | ✓ | ✓ | ✓ | 63.2 | 77.4 |
| Clustering+ConsLearn | ✓ | ✓ | ✓ | ✓ | 64.5 | 78.1 |

Table 5: Ablation studies of our proposed method on the unsupervised person re-ID task with DukeMTMC-reID. Unlike the baseline, our clustering generates pseudo labels according to features from a view of the same images and use the same labels for two encoded views to optimize model.

re-ID task. In addition, as the last line of Table 3, the performance of our method (w/o DDL) is worse than that of our method, which demonstrates that our method benefit from the single visual consistency of the same image’s different views.

Next, we investigate the effect of erased area on accuracy by changing the value of α and β . The upper part of Table 4 summaries the experimental results. From these results, we obtain the best performance with $\alpha = 0.4$ and $\beta = 0.3$ for lower-level layers. Meanwhile, when the erased area is greatly reduced (*i.e.*, $\alpha = 0.2$ and $\beta = 0.1$), 8.5% mAP and 5.1% top-1 decreases are observed. This is because the model hard capture the different semantic information of the object. Furthermore, given that higher-level feature is semantic and appearance diversity, we also reduce the size of erased area when DDL is plugged in high-level layers. The results are reported in the lower part of Table 4, while the findings are still the same as before.

Clustering. We set the model as the baseline when training the network using only the traditional classification component. To verify the effectiveness of our clustering, we conduct extensive ablation studies. From experimental results in the upper part of Table 5, it can be easily observed that the performance of our clustering is worse than that of the baseline model. The main reason is that the clustering (w/o ConsLearn) focus on local detailed feature and thus the learned features from different data flows contains different information, leading to different clustering results. However, our clustering share the same pseudo label for them. When consistency learning is also conducted (the lower part of Table 5), our clustering is greatly improved and surpass the baseline model with ConsLearn (Baseline+ConsLearn) by margins (mAP=1.3% and top-1=0.7%). This indicates that our clustering begins to ignores low-level features and focus on semantic information with the help of ConsLearn. In this way, our clustering further enhance the visual consistency by using the same cluster for two encoded features. Additionally, the softmax-triplet loss also improve the per-

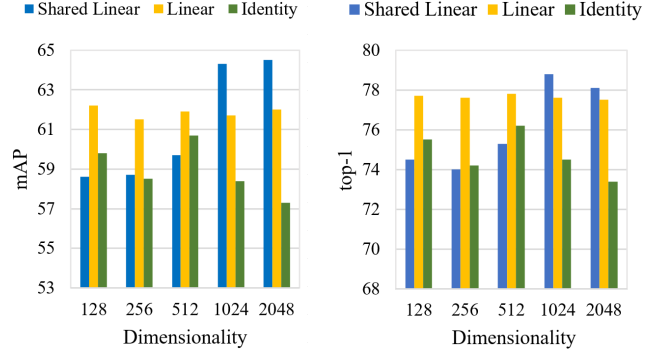


Figure 3: Evaluation results of representations with different projection heads and various dimensions.

| Method | Parameter | mAP | top-1 | top-5 |
|--------------|--|------|-------|-------|
| Ours (w/ M) | $(\theta^{(t)})$ | 64.5 | 78.1 | 87.8 |
| | $(\theta^{(t-1)})$ | 63.7 | 78.4 | 87.6 |
| | $(\theta^{(t-1)}, \theta^{(t)})$ | 63.9 | 77.6 | 87.7 |
| | $(\theta^{(t-2)}, \theta^{(t-1)}, \theta^{(t)})$ | 63.9 | 78.2 | 87.7 |
| Ours (w/o M) | N/A | 59.6 | 74.6 | 85.2 |

Table 6: Evaluation results of the temporally averaging model under different update mechanism. M: the temporal averaging model. $(\theta^{(t-1)}, \theta^{(t)})$: the averaging model is updated as $\theta_e^{(t)} = \zeta \theta_e^{(t-1)} + \frac{1-\zeta}{2} \theta^{(t-1)} + \frac{1-\zeta}{2} \theta^{(t)}$, and others are similar.

formance of our clustering method, which demonstrates the effectiveness of softmax-triplet loss in our proposed framework.

Pretext task. As showed in Table 5, the baseline model results in much lower performance than our final method. A key reason is that the baseline model mainly focuses on the local detailed features to optimize the target task of re-ID while discarding meaningful semantic feature. As a pretext or base task, consistency learning is integrated into the baseline model, abbreviated as “Baseline + ConsLearn”. Under this setting, the baseline obtain the obvious improvement (mAP=11.5% and top-1=6.5%), which further demonstrates the importance of adopting LearnCons as pretext task.

Momentum update mechanism. The momentum-based averaging model allows us to enforce the temporal consistency over network model at different iterations without additional model parameter. To investigate its effectiveness, we conduct ablation studies by directly use one networks current-iteration output as feature distribution, which is abbreviated as “Ours (w/o M)”. As shown in Table 6, “Ours (w/ M)” consistently improves the results over “Ours (w/o M)”, which represents our method without temporal consistency based on averaging model. The qualitative re-

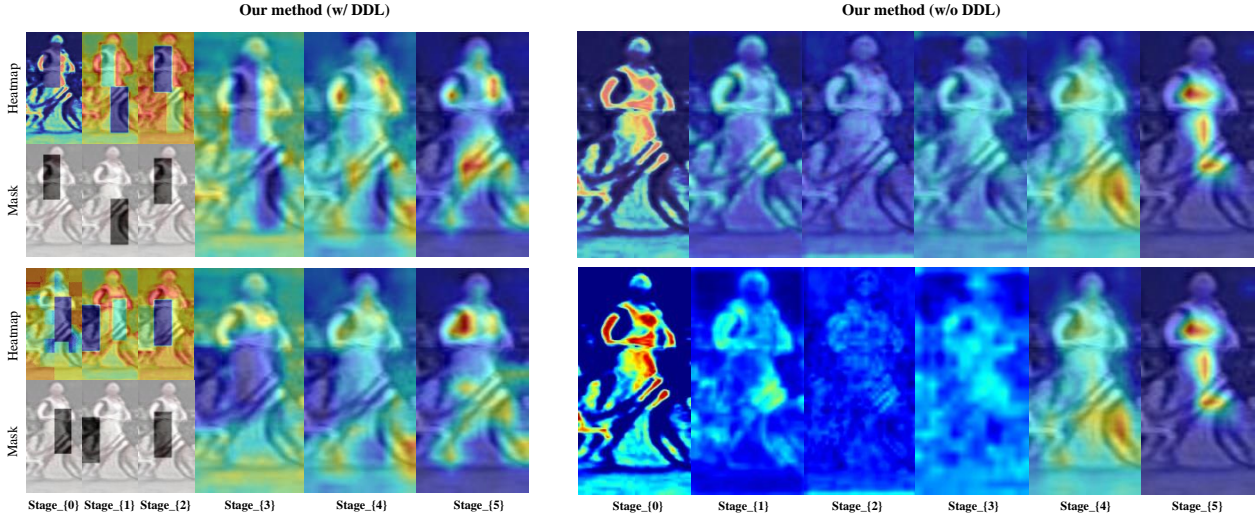


Figure 4: The dropmask and heatmap at different layers of ResNet50 [19] over two encoded features (*i.e.*, v_1 and v_2).

sults demonstrates that the necessary of temporal consistency and the single consistency obtained by model at different stages has different effects on our results.

Projection head. We then study the importance of the linear projections, *i.e.*, $f(\cdot)$ and $g(\cdot)$. Figure 3 reports evaluation results using three different architectures for the projection heads: (1) identity mapping; (2) linear projection; (3) shared linear projection for $f(\cdot)$ and $g(\cdot)$. We observe that two kinds of linear projection are obviously better than no projection (*i.e.*, identity mapping), especially for the large output dimensions (*e.g.*, 2048 in this paper). This indicate that, by using two projections, more information can be formed and maintained in u_i and \tilde{u}_i , $i=1,2$. Furthermore, the performance of shared linear becomes better as output dimensions increases and outperform normal linear with large dimensions (*e.g.*, 1024 and 2048 in this paper), which demonstrates that shared linear projection can obtain more information that is useful for two tasks.

4.4. Discussions

From the perspective of representation learning, our method integrate disparate visual percepts into persistent entities and underlie visual reasoning in feature space. As shown in the left of Figure 4, the network model (w/ DDL) no longer pays attention to some semantic parts at early stages when they are occluded. However, at later stages, the predicted target regions of training image are backtraced to the initial information by using the information of the other view regardless of losing the target on a view. Finally, the heatmap extracted from model almost highlight the entire region of the person. This indicates that the ability of model to predict the missing patch of feature maps are enhanced, inching the two different features toward consistency. On

the contrary, the right of Figure 4 shows the model (w/o DDL) only focus on the most discriminative part of object, not the entire object. In addition, unlike the pervious clustering, our clustering treats the same pseudo labels as ground truth labels for two encoded views to bootstrap the discriminative ability of network model.

Our proposed framework is trained with both unsupervised clustering and representation learning. In this way, our method can separate the images into semantic clusters, where images within the same cluster belong to the semantic classes and images in different clusters are semantically dissimilar. Since self-supervised representation learning is task-agnostic during training, they often have to focus on the feature information, which is unrelated to the current target task. Indeed, in our method, the clustering induces network model to capture feature representation that concentrates on the target task of re-ID. Meanwhile, consistency learning encourages clustering to obtain semantically meaningful features rather than relying on low-level features.

5. Conclusion

In this paper, we present a new approach for unsupervised person re-identification (re-ID) by combining clustering and consistency learning. As a target task, clustering learning trains a deep neural network using generated pseudo-labels and concentrates on current task of re-ID. As a pretext task, consistency learning requires semantic understanding and induces clustering to obtain semantically meaningful features rather than depending on low-level features. Experimental results show that our method achieves significant improvements over a variety of unsupervised or domain adaptive re-ID tasks.

References

- [1] Philip Bachman, R Devon Hjelm, and William Buchwalter. Learning representations by maximizing mutual information across views. *arXiv preprint arXiv:1906.00910*, 2019.
- [2] Slawomir Bak, Peter Carr, and Jean-Francois Lalonde. Domain adaptation through synthesis for unsupervised person re-identification. In *Proceedings of the European Conference on Computer Vision*, pages 189–205, 2018.
- [3] Yue Cao, Zhenda Xie, Bin Liu, Yutong Lin, Zheng Zhang, and Han Hu. Parametric instance classification for unsupervised visual feature learning. *arXiv preprint arXiv:2006.14618*, 2020.
- [4] Mathilde Caron, Ishan Misra, Julien Mairal, Priya Goyal, Piotr Bojanowski, and Armand Joulin. Unsupervised learning of visual features by contrasting cluster assignments. *arXiv preprint arXiv:2006.09882*, 2020.
- [5] Ting Chen, Simon Kornblith, Mohammad Norouzi, and Geoffrey Hinton. A simple framework for contrastive learning of visual representations. In *International Conference on Machine Learning*, pages 1597–1607. PMLR, 2020.
- [6] Yanbei Chen, Xiatian Zhu, and Shaogang Gong. Instance-guided context rendering for cross-domain person re-identification. In *Proceedings of the IEEE International Conference on Computer Vision*, pages 232–242, 2019.
- [7] De Cheng, Yihong Gong, Sanping Zhou, Jinjun Wang, and Nanning Zheng. Person re-identification by multi-channel parts-based cnn with improved triplet loss function. In *Proceedings of the IEEE Conference on Computer Vision and Pattern Recognition*, pages 1335–1344, 2016.
- [8] Jia Deng, Wei Dong, Richard Socher, Li-Jia Li, Kai Li, and Li Fei-Fei. Imagenet: A large-scale hierarchical image database. In *Proceedings of the IEEE Conference on Computer Vision and Pattern Recognition*, pages 248–255. IEEE, 2009.
- [9] Weijian Deng, Liang Zheng, Qixiang Ye, Guoliang Kang, Yi Yang, and Jianbin Jiao. Image-image domain adaptation with preserved self-similarity and domain-dissimilarity for person re-identification. In *Proceedings of the IEEE Conference on Computer Vision and Pattern Recognition*, pages 994–1003, 2018.
- [10] Terrance DeVries and Graham W Taylor. Improved regularization of convolutional neural networks with cutout. *arXiv preprint arXiv:1708.04552*, 2017.
- [11] Martin Ester, Hans-Peter Kriegel, Jörg Sander, Xiaowei Xu, et al. A density-based algorithm for discovering clusters in large spatial databases with noise. In *KDD*, volume 96, pages 226–231, 1996.
- [12] Hehe Fan, Liang Zheng, Chenggang Yan, and Yi Yang. Unsupervised person re-identification: Clustering and fine-tuning. *ACM Transactions on Multimedia Computing, Communications, and Applications*, 14(4):1–18, 2018.
- [13] Yang Fu, Yunchao Wei, Guanshuo Wang, Yuqian Zhou, Honghui Shi, and Thomas S Huang. Self-similarity grouping: A simple unsupervised cross domain adaptation approach for person re-identification. In *Proceedings of the IEEE Conference on Computer Vision and Pattern Recognition*, pages 6112–6121, 2019.
- [14] Yixiao Ge, Dapeng Chen, and Hongsheng Li. Mutual mean-teaching: Pseudo label refinery for unsupervised domain adaptation on person re-identification. *arXiv preprint arXiv:2001.01526*, 2020.
- [15] Jean-Bastien Grill, Florian Strub, Florent Altché, Corentin Tallec, Pierre H Richemond, Elena Buchatskaya, Carl Doersch, Bernardo Avila Pires, Zhaohan Daniel Guo, Mohammad Gheshlaghi Azar, et al. Bootstrap your own latent: A new approach to self-supervised learning. *arXiv preprint arXiv:2006.07733*, 2020.
- [16] Raia Hadsell, Sumit Chopra, and Yann LeCun. Dimensionality reduction by learning an invariant mapping. In *2006 IEEE Computer Society Conference on Computer Vision and Pattern Recognition*, volume 2, pages 1735–1742. IEEE, 2006.
- [17] Tengda Han, Weidi Xie, and Andrew Zisserman. Self-supervised co-training for video representation learning. *arXiv preprint arXiv:2010.09709*, 2020.
- [18] Kaiming He, Haoqi Fan, Yuxin Wu, Saining Xie, and Ross Girshick. Momentum contrast for unsupervised visual representation learning. In *Proceedings of the IEEE/CVF Conference on Computer Vision and Pattern Recognition*, pages 9729–9738, 2020.
- [19] Kaiming He, Xiangyu Zhang, Shaoqing Ren, and Jian Sun. Deep residual learning for image recognition. In *Proceedings of the IEEE Conference on Computer Vision and Pattern Recognition*, pages 770–778, 2016.
- [20] Olivier Henaff. Data-efficient image recognition with contrastive predictive coding. In *International Conference on Machine Learning*, pages 4182–4192. PMLR, 2020.
- [21] Alexander Hermans, Lucas Beyer, and Bastian Leibe. In defense of the triplet loss for person re-identification. *arXiv preprint arXiv:1703.07737*, 2017.
- [22] Xin Jin, Cuiling Lan, Wenjun Zeng, Zhibo Chen, and Li Zhang. Style normalization and restitution for generalizable person re-identification. In *Proceedings of the IEEE Conference on Computer Vision and Pattern Recognition*, pages 3143–3152, 2020.
- [23] Alex Krizhevsky, Ilya Sutskever, and Geoffrey E Hinton. Imagenet classification with deep convolutional neural networks. *Communications of the ACM*, 60(6):84–90, 2017.
- [24] Minxian Li, Xiatian Zhu, and Shaogang Gong. Unsupervised person re-identification by deep learning tracklet association. In *Proceedings of the European Conference on Computer Vision*, pages 737–753, 2018.
- [25] Wei Li, Xiatian Zhu, and Shaogang Gong. Harmonious attention network for person re-identification. In *Proceedings of the IEEE Conference on Computer Vision and Pattern Recognition*, pages 2285–2294, 2018.
- [26] Yu-Jhe Li, Ci-Siang Lin, Yan-Bo Lin, and Yu-Chiang Frank Wang. Cross-dataset person re-identification via unsupervised pose disentanglement and adaptation. In *Proceedings of the IEEE International Conference on Computer Vision*, pages 7919–7929, 2019.
- [27] Yutian Lin, Xuanyi Dong, Liang Zheng, Yan Yan, and Yi Yang. A bottom-up clustering approach to unsupervised person re-identification. In *Proceedings of the AAAI Conference on Artificial Intelligence*, volume 33, pages 8738–8745, 2019.

- [28] Yutian Lin, Lingxi Xie, Yu Wu, Chenggang Yan, and Qi Tian. Unsupervised person re-identification via softened similarity learning. In *Proceedings of the IEEE Conference on Computer Vision and Pattern Recognition*, pages 3390–3399, 2020.
- [29] Jiawei Liu, Zheng-Jun Zha, Di Chen, Richang Hong, and Meng Wang. Adaptive transfer network for cross-domain person re-identification. In *Proceedings of the IEEE Conference on Computer Vision and Pattern Recognition*, pages 7202–7211, 2019.
- [30] Lei Qi, Lei Wang, Jing Huo, Luping Zhou, Yinghuan Shi, and Yang Gao. A novel unsupervised camera-aware domain adaptation framework for person re-identification. In *Proceedings of the IEEE International Conference on Computer Vision*, pages 8080–8089, 2019.
- [31] Ergys Ristani, Francesco Solera, Roger Zou, Rita Cucchiara, and Carlo Tomasi. Performance measures and a data set for multi-target, multi-camera tracking. In *Proceedings of the European Conference on Computer Vision*, pages 17–35. Springer, 2016.
- [32] Nitish Srivastava, Geoffrey Hinton, Alex Krizhevsky, Ilya Sutskever, and Ruslan Salakhutdinov. Dropout: a simple way to prevent neural networks from overfitting. *The journal of machine learning research*, 15(1):1929–1958, 2014.
- [33] Yonglong Tian, Dilip Krishnan, and Phillip Isola. Contrastive multiview coding. *arXiv preprint arXiv:1906.05849*, 2019.
- [34] Yonglong Tian, Chen Sun, Ben Poole, Dilip Krishnan, Cordelia Schmid, and Phillip Isola. What makes for good views for contrastive learning. *arXiv preprint arXiv:2005.10243*, 2020.
- [35] Laurens Van Der Maaten. Accelerating t-sne using tree-based algorithms. *The Journal of Machine Learning Research*, 15(1):3221–3245, 2014.
- [36] Dongkai Wang and Shiliang Zhang. Unsupervised person re-identification via multi-label classification. In *Proceedings of the IEEE Conference on Computer Vision and Pattern Recognition*, pages 10981–10990, 2020.
- [37] Xiaolong Wang, Allan Jabri, and Alexei A Efros. Learning correspondence from the cycle-consistency of time. In *Proceedings of the IEEE Conference on Computer Vision and Pattern Recognition*, pages 2566–2576, 2019.
- [38] Zhongdao Wang, Jingwei Zhang, Liang Zheng, Yixuan Liu, Yifan Sun, Yali Li, and Shengjin Wang. Cycas: Self-supervised cycle association for learning re-identifiable descriptions. *arXiv preprint arXiv:2007.07577*, 2020.
- [39] Longhui Wei, Shiliang Zhang, Wen Gao, and Qi Tian. Person transfer gan to bridge domain gap for person re-identification. In *Proceedings of the IEEE Conference on Computer Vision and Pattern Recognition*, pages 79–88, 2018.
- [40] Zhirong Wu, Yuanjun Xiong, Stella X Yu, and Dahua Lin. Unsupervised feature learning via non-parametric instance discrimination. In *Proceedings of the IEEE Conference on Computer Vision and Pattern Recognition*, pages 3733–3742, 2018.
- [41] Tong Xiao, Shuang Li, Bochao Wang, Liang Lin, and Xiaogang Wang. Joint detection and identification feature learning for person search. In *Proceedings of the IEEE Conference on Computer Vision and Pattern Recognition*, pages 3415–3424, 2017.
- [42] Zhenda Xie, Yutong Lin, Zheng Zhang, Yue Cao, Stephen Lin, and Han Hu. Propagate yourself: Exploring pixel-level consistency for unsupervised visual representation learning. *arXiv preprint arXiv:2011.10043*, 2020.
- [43] Mang Ye, Xu Zhang, Pong C Yuen, and Shih-Fu Chang. Unsupervised embedding learning via invariant and spreading instance feature. In *Proceedings of the IEEE Conference on Computer Vision and Pattern Recognition*, pages 6210–6219, 2019.
- [44] Hong-Xing Yu, Wei-Shi Zheng, Ancong Wu, Xiaowei Guo, Shaogang Gong, and Jian-Huang Lai. Unsupervised person re-identification by soft multilabel learning. In *Proceedings of the IEEE Conference on Computer Vision and Pattern Recognition*, 2019.
- [45] Hong Xing Yu, Wei Shi Zheng, Ancong Wu, Xiaowei Guo, and Jian Huang Lai. Unsupervised person re-identification by soft multilabel learning. In *Proceedings of the IEEE Conference on Computer Vision and Pattern Recognition*, 2019.
- [46] Kaiwei Zeng, Munan Ning, Yaohua Wang, and Yang Guo. Hierarchical clustering with hard-batch triplet loss for person re-identification. In *Proceedings of the IEEE Conference on Computer Vision and Pattern Recognition*, pages 13657–13665, 2020.
- [47] Yunpeng Zhai, Shijian Lu, Qixiang Ye, Xuebo Shan, Jie Chen, Rongrong Ji, and Yonghong Tian. Ad-cluster: Augmented discriminative clustering for domain adaptive person re-identification. In *Proceedings of the IEEE Conference on Computer Vision and Pattern Recognition*, pages 9021–9030, 2020.
- [48] Yunpeng Zhai, Qixiang Ye, Shijian Lu, Mengxi Jia, Rongrong Ji, and Yonghong Tian. Multiple expert brainstorming for domain adaptive person re-identification. *arXiv preprint arXiv:2007.01546*, 2020.
- [49] Xinyu Zhang, Jiwei Cao, Chunhua Shen, and Mingyu You. Self-training with progressive augmentation for unsupervised cross-domain person re-identification. In *Proceedings of the IEEE International Conference on Computer Vision*, pages 8222–8231, 2019.
- [50] Liang Zheng, Liyue Shen, Lu Tian, Shengjin Wang, Jingdong Wang, and Qi Tian. Scalable person re-identification: A benchmark. In *Proceedings of the IEEE international Conference on Computer Vision*, pages 1116–1124, 2015.
- [51] Zhun Zhong, Liang Zheng, Shaozi Li, and Yi Yang. Generalizing a person retrieval model hetero-and homogeneously. In *Proceedings of the European Conference on Computer Vision*, pages 172–188, 2018.
- [52] Zhun Zhong, Liang Zheng, Zhiming Luo, Shaozi Li, and Yi Yang. Invariance matters: Exemplar memory for domain adaptive person re-identification. In *Proceedings of the IEEE Conference on Computer Vision and Pattern Recognition*, pages 598–607, 2019.
- [53] Zhun Zhong, Liang Zheng, Zhiming Luo, Shaozi Li, and Yi Yang. Learning to adapt invariance in memory for person re-

identification. *IEEE Transactions on Pattern Analysis and Machine Intelligence*, 2020.

- [54] Yang Zou, Xiaodong Yang, Zhiding Yu, BVK Kumar, and Jan Kautz. Joint disentangling and adaptation for cross-domain person re-identification. *arXiv preprint arXiv:2007.10315*, 2020.